Title
X-ray Holography of Fast-Frozen Hydrated Biological Samples

Author
Lindaas, S.

Publication Date
1997

LBNL-39523
UC-410

ERNEST ORLANDO LAWRENCE
BERKELEY NATIONAL LABORATORY

X-ray Holography of Fast-Frozen Hydrated Biological Samples

S. Lindaas, B. Calef, K. Downing, M. Howells,
C. Magowan, D. Pinkas, and C. Jacobsen
Accelerator and Fusion Research Division

November 1996
Published as
a chapter in
X-ray Microscopy and Spectromicroscopy,
J. Thieme, G. Schmahl,
E. Umbach, and
D. Rudolph, Eds.,
Springer-Verlag,
Heidelberg, Germany, 1996

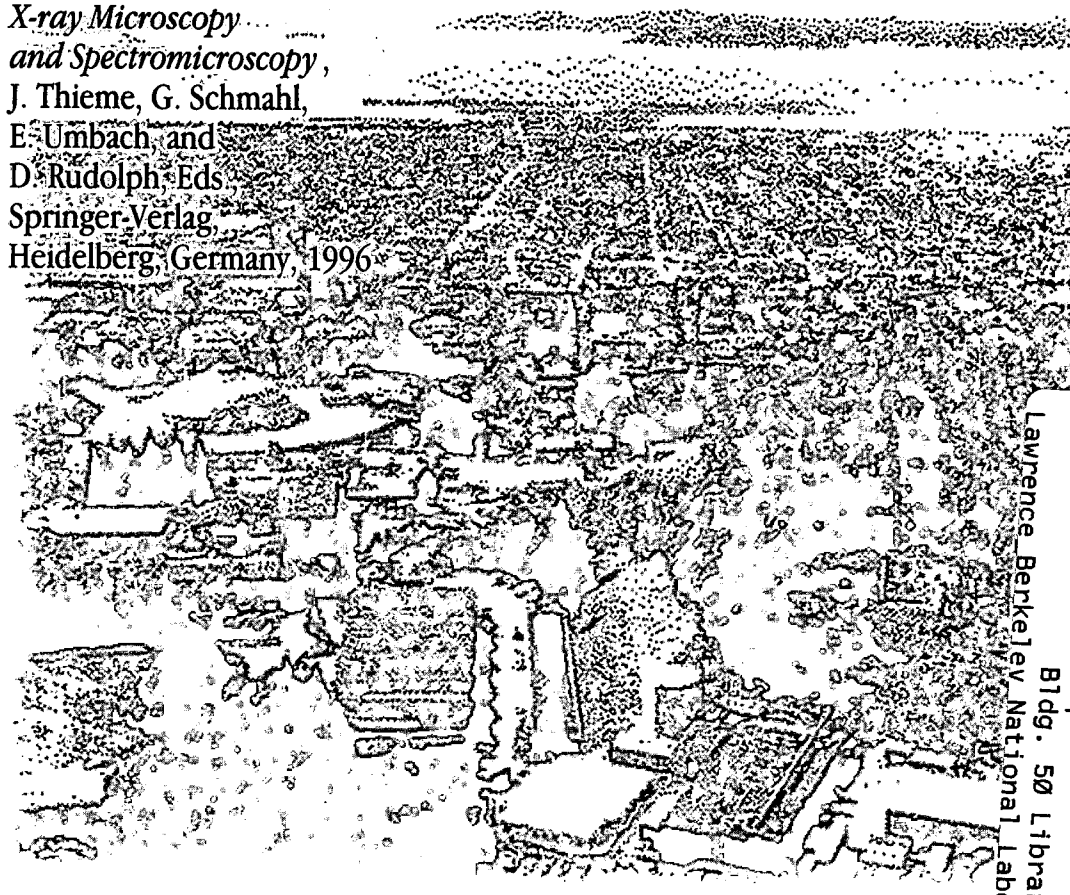

DISCLAIMER

LBNL-39523
LSBL-354
UC-410

X-RAY HOLOGRAPHY OF FAST-FROZEN HYDRATED BIOLOGICAL SAMPLES*

S. Lindaas, B. Calef, K. Downing, M. Howells, C. Magowan, D. Pinkas
Advanced Light Source
Accelerator & Fusion Research Division
Ernest Orlando Lawrence Berkeley National Laboratory
University of California, Berkeley, California 94720

C. Jacobsen
Physics Department
State University of New York
Stony Brook, NY 11794

*This work was supported by the Director, Office of Energy Research, Office of Basic Energy Sciences, Materials Sciences Division, of the U.S. Department of Energy, under Contract No. DE-AC03-76SF00098.

X-ray Holography of Fast-Frozen Hydrated Biological Samples

S. Lindaas, B. Calef, K. Downing, M. Howells, C. Magowan, D. Pinkas,
Lawrence Berkeley National Laboratory, Cyclotron Rd, Berkeley CA 94720, USA.
C. Jacobsen,
Physics Department, State University of New York, Stony Brook, NY 11794, USA.
E-mail: lindaas@afm1.lbl.gov

1. Introduction

Although x-ray holography has a long history,[11] it is only in recent times that short-wavelength lasers and undulator x-ray sources have opened the possibility for competitive imaging performance. Experiments using the in-line (Gabor) geometry have been favored by most groups and have been carried out at Orsay,[12] Brookhaven,[9] Livermore,[31] Tsukuba,[34] Chilton,[32] Osaka[27] and Grenoble[28] while the Fourier-transform geometry has been developed at Brookhaven.[23] Submicron resolution has been reported by the Orsay group[12] and by some of the present authors working at Brookhaven.[10] These holographic schemes all operated in or near the water window and were mostly conceived as technical developments toward imaging of natural biological material. Their motivations were mostly the practical simplicity of the hologram recording process, which is similar to contact imaging, and the fact that such recordings can be made to deliver both the amplitude and phase images. The chief disadvantages are that holography provides no escape from the large radiation dose that is required by all x-ray and electron imaging methods and that the in-line style of holography produces an inherent corruption to the desired image known as the twin image. We have discussed the question of how to exploit the potential of x-ray holography in light of these disadvantages in an earlier paper[18] and have concluded that part of the solution is to cool the sample to cryogenic temperatures. Under this condition, features as small as 5 nm remain intact at doses of up to

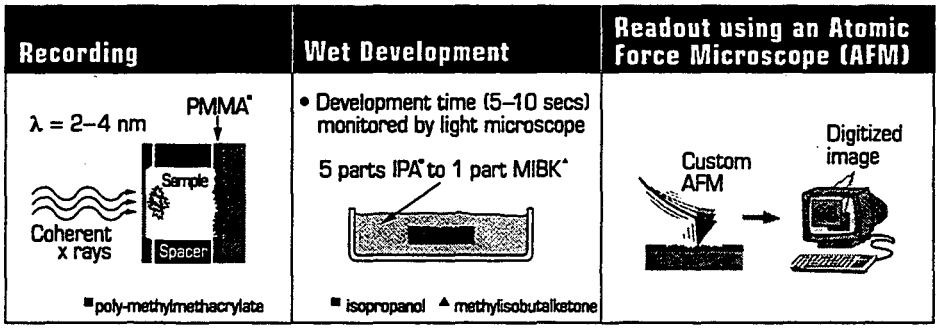

Fig. 1. The photoresist PMMA is used to record the hologram which consists of the interference pattern formed by the plane reference wave and the wave diffracted from the sample. The sample-photoresist spacing (typically 400μm) is determined in the reconstruction step (see Sec. VII). Some of the exposed polymer suffers mass loss during irradiation (self development) and more is later removed deliberately during wet development. Light development is necessary to avoid "washing out" low-contrast fringes.[33] The photoresist relief map (corresponding to incident x-ray intensity) is measured/digitized using our specially-made atomic-force microscope.[18, 19]

10^8 Gray which thus allows a tilt series containing scores of holographic images to be taken.

In this paper we describe the design and operation of a new experimental apparatus with which we have recorded a number of holograms of natural wet biological samples at liquid nitrogen temperature. We also report how, after digitizing the holograms using an atomic-force microscope,[18] we have addressed the problem of how to make a numerical reconstruction of the image. We discuss the nature of the twin image problem in the language of the theory of convex sets and show that standard reconstruction algorithms are effective in certain cases but inefficient in others.

2. In-line Holography

The procedure that we have used for recording and readout of the holograms is outlined in Figure 1 and in our earlier publications.[18]

3. Description of Experimental Apparatus

We have designed and built an experimental apparatus to enable us to record holograms at liquid-nitrogen temperature. Wherever possible we have taken advantage of commercially available systems developed for the electron microscopy community and have thereby obtained proven hardware for preparing the sample and loading it into the vacuum. In particular, we adapted a transmission electron microscope (TEM) cryo-holder (Fig. 2) designed to hold a 3 mm diameter TEM grid so that it could accommodate a relatively thick "package" consisting of the sample-grid, a spacer (≈300 μm) and a 500-μm-thick substrate covered with photoresist. The sample was cooled via a cold finger extending from the liquid-nitrogen dewar which allowed a temperature of -160°C to be easily maintained at the sample as long as the dewar was partially filled. The cryo-holder was also equipped with a heater which was useful in de-icing the tip between sample changes and could also be used as a means to freeze dry samples in vacuum. A thermocouple located next to the sample region allowed the temperature to be continuously monitored.

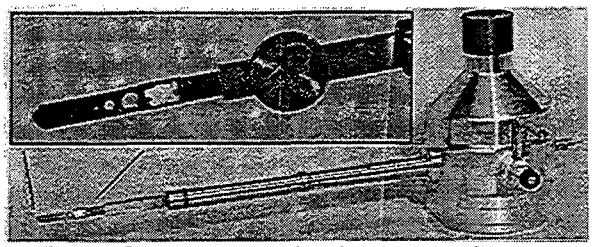

Fig. 2. Cryo-sample holder showing sample area.

We also purchased the TEM airlock mechanism that mated with the cryo-sample holder and designed an interface for mounting it on an "xyzθ" stage[15] which allowed the sample to be accurately positioned at the center of our chamber. The whole system was capable of 10^{-9} torr although in the experiments reported here the chamber pressure was about 10^{-5} torr. The cryo-sample holder and cryo work station plus the airlock were designed to enable samples that have been fast frozen to liquid-nitro-

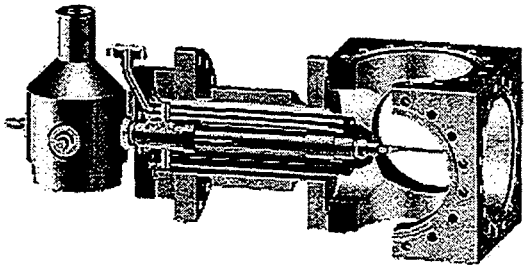

Fig. 3. Schematic of cryo-holography chamber with cut-away of the airlock and its interface.

gen temperature to be stored as long as needed at that temperature and then transferred into a vacuum chamber without warming above -160°C (at which temperature damage due to ice crystal growth would begin to occur). A cut-away diagram of the apparatus is shown in Fig. 3 and a photograph of it in place on beamline X1A at the National Synchrotron Light Source (NSLS) at Brookhaven National Laboratory is shown in Figure 4.

The sample positioning system also included a stereo microscope with a 7 inch working distance. By this means one could look at the cryo-sample holder with the x-ray beam on via an x-ray transparent mirror (Al coated on a Si_3N_4 window) placed at 45 degrees to the beam. Phosphor was placed on the cryo-holder shutter (see Figure 2) so that targeting of the beam on to a chosen sample area could be accomplished by using the microscope reticule.

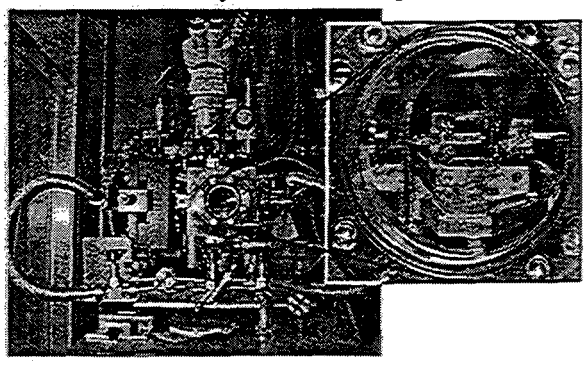

Fig. 4. Cryo-holography chamber setup at X1A. The cryo-sample holder is inserted from the left and the stereo microscope used to align the sample via the alignment mirror (see inset).

4. Sample Preparation

The samples used in these experiments were red blood cells infected with the *Plasmodium falciparum* malaria parasite which were made by the Hematopoiesis/Mammary Cell Biology Group at the Lawrence Berkeley National Laboratory (LBNL). The size of these cells made them well suited for x-ray holography and preparation techniques had already been worked out for imaging them in a transmission x-ray microscope.[24]

Infected red blood cells were cultured *in vitro* as previously described.[29] Mature trophozoite stage infected erythrocytes were enriched to >80% by flotation in 0.5% gelatin[25] and fixed with 1% glutaraldehyde. All of the pathology and mortality associated with *Plasmodium falciparum* malaria is due to the blood stages of infection. The trophozoite is the developmental stage which is actively metabolizing hemoglobin and synthesizing new proteins that associate with the host erythrocyte membrane to alter its morphology, antigenicity, and function.[1, 13, 21, 30]

The cell culture was diluted till approximately one or two cells occupied each $(40\ \mu m)^2$ grid area in test preparations. Using the fast-freezing workstation at Donner Laboratory (LBNL) we prepared frozen samples from this diluted cell culture. This workstation used immersion cooling[4] (via a spring-loaded plunger into liquid ethane) and was equipped to control the humidity around the sample to avoid sample dehydration, which can happen very quickly. The cryo-samples were placed under liquid nitrogen in modified storage trays, designed for electron-microscope grids, and then shipped to the Brookhaven using the "dry-shipper" type of cryogenic container.

5. Experimental Procedure

The fast frozen sample, the sample holder, the resist substrate and spacer were all introduced into the liquid-nitrogen-temperature environment of the cryo-work station and as-

sembled there. Once in place the resist-spacer-sample package was covered with the shutter to minimize ice build-up during the transfer. The whole cryo-work station was then moved to the beam-line area and the cryo holder was inserted into the airlock.

The x-ray beam was then aligned over region of interest using the stereo microscope and the package was exposed. Using λ=2.4nm x-rays with $\lambda/\Delta\lambda \geq 150$ and a spatial coherence footprint of better than $(40\mu m)^2$, we had 3×10^8 photons/μm^2 incident on the sample. For a sample with a 10μm thick water/ice layer, this gives about 10^8 photons/μm^2 on the resist and a sample dose of approximately 2×10^6 Grays. The exposure was monitored by photodiode measurements of the beam and optical-microscope examination of the self-developed resist. The magnified atomic-force-microscope image of the hologram is shown in Figure 5.

Once the hologram was digitized, processing was carried out, using our own software package written in IDL, on a Pentium-Pro based computer with 256 Mbytes of RAM running Linux (version 2.0.0). The basic propagation operation between the hologram and object plane took about one minute for a 2048^2-pixel hologram and the corresponding speed of the twin-image algorithm was about 1.4 days per thousand iterations

6. Results

We have recorded a number of holograms of natural, wet samples that were fast frozen in a manner consistent with producing amorphous ice and maintained at cryogenic temperature until after imaging. The fully processed version of the one we chose for our studies of twin-image suppression is shown in Figure 5. By calculation of the power spectrum we have determined that there is no white-noise roll off so that information is apparently recorded in the photoresist to better than 30 nm. A reconstructed image obtained by the numerical equivalent of illumination of the hologram with the original reference wave is shown in Figure 6 (the object-to-hologram distance was found by software to be 425 μm). The fringe artifacts due to the twin-image signal are readily apparent in the reconstructed image and we discuss this issue more fully in the next section.

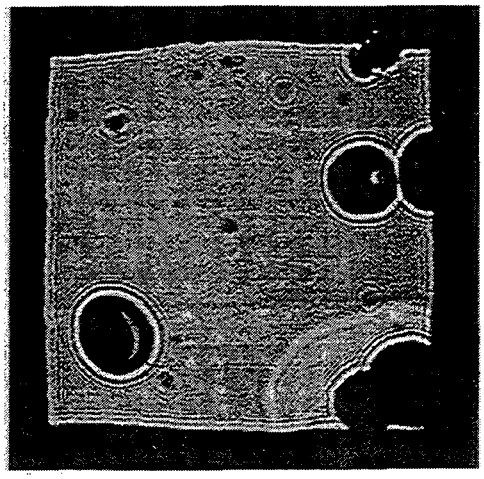

Fig. 5. Hologram of malaria infected red blood cells. AFM readout: $(21nm)^2$ pixels in a $(2048)^2$ array.

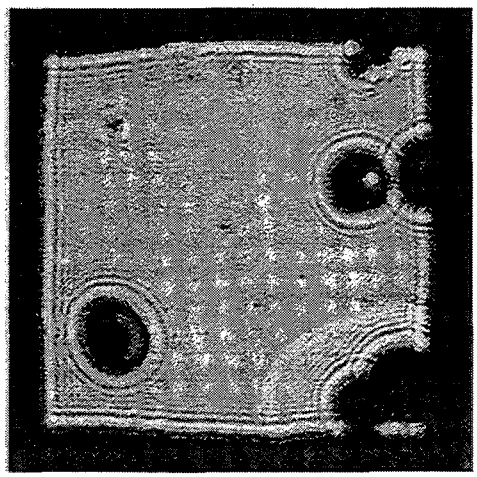

Fig. 6. Numerically reconstructed image. The focus was found to be at z=425μm.

7. The twin-image signal and its suppression

A hologram is formed when a complex wavefield $a(\mathbf{x})$ scattered by the sample and a coherent reference wavefield $r(\mathbf{x})$ are made to interfere, registering an intensity $I(\mathbf{x}) = |r(\mathbf{x}) + a(\mathbf{x})|^2$ in the x plane. For an axial-plane-wave reference beam (Figure 1), r is a real constant which we take to be unity. Then

$$I(\mathbf{x}) = 1 + |a(\mathbf{x})|^2 + a(\mathbf{x}) + a^*(\mathbf{x}) \tag{1}$$

The four terms are known as the zero-order, intermodulation, virtual image and real image terms respectively. To calculate $a(\mathbf{x})$ suppose the object is represented by a two-dimensional complex transparency function $T(\mathbf{x}')$ which we prefer to write as $1 - A(\mathbf{x}')$ where $A(\mathbf{x}')$ is the complex *absorbency*. We can express the diffracted wavefield at distance z downstream by means of a propagation operator P_z with the following properties: $P_z(1) = 1$, $P_z^* = P_{-z}$, $P_z P_{-z} = 1$, $P_{z_1} P_{z_2} = P_{z_2} P_{z_1} = P_{z_1+z_2}$. This operator represents the action of the diffraction integral on the initial wavefield and we have implemented it in software[20]. In terms of P_z the field $1 + a(\mathbf{x})$ at the hologram is $P_z[1 - A(\mathbf{x}')]$ and

$$I(\mathbf{x}) = 1 + \left|P_z[A(\mathbf{x}')]\right|^2 - P_z[A(\mathbf{x}')] - P_z^*\left[A^*(\mathbf{x}')\right]. \tag{2}$$

Evidently the quantity $P_z(-A(\mathbf{x}')$ is equivalent to the wavefield $a(\mathbf{x})$ used above.

The process of reconstructing the virtual image consists of illuminating the hologram $I(\mathbf{x})$ with a unit plane wave and backpropagating a distance z. In a numerical calculation, this leads to a complex amplitude distribution $A_1(\mathbf{x}')$

$$A_1(\mathbf{x}') = P_z^*[I(\mathbf{x})] = 1 + P_z^*\left|P_z[A(\mathbf{x}')]\right|^2 - A(\mathbf{x}') - P_{2z}^*\left[A^*(\mathbf{x}')\right]. \tag{3}$$

Therefore, with a reference wave of *exactly* unity, it is $-A(\mathbf{x}')$ that we reconstruct in the object plane along with unwanted signals derived from the intermodulation term and the out-of-focus real image (the twin-image). The so-called twin-image problem of in-line holography is to extract the object A given only the hologram.

In some applications of in-line holography, the intermodulation term can be neglected. In such cases the cosines of the phases can be inferred from the hologram and particular approaches to the twin-image problem become appropriate.[14, 22] However, examination of equation (3) shows that neglect of the intermodulation term can only be justified when $|A(\mathbf{x}')|^2 << 1$. For this to be true the sample would have to be both a weak scatterer and a weak absorber and this is certainly not something we can normally assume in x-ray microscopy.

The twin-image problem is a member of a class of phase problems that arise commonly in optics. The class includes, image restoration from amplitude, for example in speckle interferometry,[3] Michelson stellar interferometry,[7] defocused pairs[2] or image-plane-diffraction-plane pairs,[26] the design of computer-generated holograms[5] and many others. The general problem is to reconstruct a complex wave function given incomplete information about the function itself and the magnitude of its transformation by a known linear operator.

In the above notation, the scenario of principal interest is that (i) we know that A is different from zero only within a certain region of the object plane (its support) and (ii) we know that the magnitude of $P_z(1-A)$ equals $\sqrt{I}$. There are two algorithms in widespread use for solving this type of problem: the error-reduction algorithm due to

Gerchberg and Saxton[6] and the input-output algorithm of Fienup.[5] Their general structure is as follows: start in the hologram plane with the amplitudes equal to $\sqrt{I}$ and guesses for the phases. Next transform (using P_{-z}) to the object plane and impose one or more constraints derived from a knowledge of the object or its support (Gerchberg-Saxton) and from earlier iterations (Fienup). Finally transform back (using P_z) to the hologram plane, reimpose the hologram amplitudes and repeat. A detailed description of these algorithms together with practical advice for their application to optical problems is given by Dainty and Fienup.[3]

A useful insight into the behavior of image recovery algorithms such as Gerchberg-Saxton is provided by a geometrical interpretation developed by Youla.[36] The images under consideration, with $M=N\times N$ pixels, say, are regarded as points in an M-dimensional space. The effect of a constraint is then to limit the image to lie within a certain subset of the space. The support constraint ((i) above), for example, restricts the image to the set of points for which certain of the M coordinates are prescribed to be zero. In the same language the hologram constraint requires the image to be a member of the set of all images the amplitude of whose transform (by P_z) is equal to the measured value $\sqrt{I}$. There can be any number of such constraint sets and the solution, if it exists, must be in the set whose members are common to all of the constraint sets, *i. e.* their intersection.

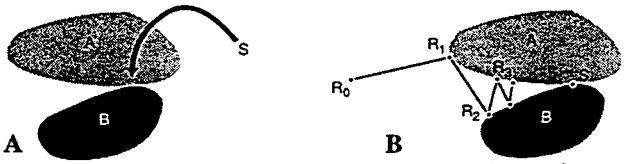

Fig. 7. Convex sets and possible unique solution *S*.

Suppose we want to find an image satisfying two constraints. This is represented pictorially in Figure 7(a). If a unique solution exists, then there will be just one image that is a member of both constraint sets, namely the point S in the figure. The procedure for finding the point S is illustrated in Figure 7(b). Let the starting image, which may be a guess, be represented by R_0. Let the projection of R_0 on the set A be R_1 (*i e* R_1 is the point in A closest to R_0). Let R_2 be the projection of R_1 on to B and so on. If the constraint sets A and B represent the support and hologram constraints respectively then the scheme in Figure 7 is precisely Gerchberg-Saxton.

Fig. 8. Unfavorable constraint set shapes.

One can see in a general way from Figure 8 that if the shape of the constraint set is unfavorable, the alternating-projections procedure may converge to a local minimum rather than to the true solution at point S. The conditions needed to avoid this can be understood by means of the theory of convex sets[8, 17]. A set is said to be convex if for any points $\mathbf{X}_1$ and $\mathbf{X}_2$ in the set the point

$$\mathbf{Y} = \lambda\mathbf{X}_1 + (1-\lambda)\mathbf{X}_2 \quad (0 \le \lambda \le 1) \tag{4}$$

is also in the set, where $\mathbf{Y}$ is called the convex combination of $\mathbf{X}_1$ and $\mathbf{X}_2$. In other words a set is convex if for any two points in the set, the line segment joining the two points is also in the set. One can see from Figure 8 that it is plausible that strong convergence to the correct solution should occur in the event that all the constraint sets are convex and this has been shown rigorously by Youla.[35] It can also be shown[3] that the

Gerchberg-Saxton procedure converges weakly, *i e* does not diverge, even if the sets are not convex. This means that for nonconvex sets, the procedure may converge or it may stagnate.

This leads us to consider whether or not the constraint sets we are interested in are convex and we consider the following four cases:

Constraint set=set of all images with:	Convex ?	Argument
certain prescribed pixels=0 (support)	Yes	If prescribed components of $\mathbf{X}_1$ and $\mathbf{X}_2$ are zero, then (by (4)) those of every Y must be also, so the Y's are in the set.
given phases	Yes	Complex numbers with given phase lie on a radius vector of the Argand plane, thence also their convex combinations.
given real parts	Yes	Complex numbers with given real part lie on an ordinate of the Argand plane, thence also their convex combinations.
given amplitudes	No	Complex numbers with given amplitude lie on a circle in the Argand plane but their convex combinations do not.

This explains why restoration from phase is easier than from amplitude and why neglect of the intermodulation term is helpful (because then eq. (2) yields the real part of $P_Z(A(\mathbf{x}'))$). However, since the hologram constraint set is nonconvex, the convergence of the algorithms we are using is not assured.

We have used the Gerchberg-Saxton and Fienup algorithms to seek solutions to the twin-image problem of in-line x-ray holography taking the hologram in Figure 5 as an example. Our experience in applying the algorithms to both experimental and model data is as follows:

1. The algorithms work best if used in combination rather than separately. Best results have been obtained by using a fixed number of iterations (10-100) of each algorithm in turn.
2. Model objects that are sparse enough for in-line holography to work (>80% empty, say), reconstruct with essentially no error (Figure 9) and this remains true even when realistic amounts of random noise are added.
3. The number of iterations involved in may be quite large ($>10^3$) and features in

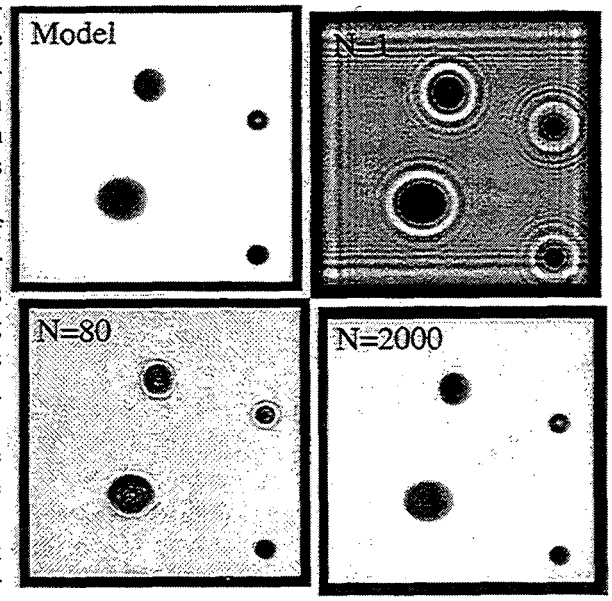

Fig. 9. The model objects shown, in a $(28\mu m)^2$ field, were used to test the twin-image suppression algorithm. The reconstructed hologram after N=1 iteration shows substantial twin-image corruption. After N=80 iterations the small objects has been recovered but the large (6μm) object and the smaller donut-shaped object are not recovered until N=2000 iterations.

the centers of the largest objects require more iterations to reach a solution than those in smaller ones (see Figure 9). It appears that this is due to the diminished effectiveness of the support constraint for features that scatter little energy into the region governed by the constraint due to their distance from the support boundary.

4. For experimental data (when only the hologram is given) there are difficulties in determining the best support boundary and in allowing for spatial variations in the incoming beam intensity. At the present time we refine the support boundary manually at least once during progress toward a solution and determine the beam intensity from a quadratic surface determined by fitting in the open areas.
5. For the reasons that were discussed in 3. above the algorithm tends to stagnate (that is it becomes trapped in a "tunnel") for thousands of iterations for the largest objects in our images which are blood cells about 7-8 μm wide. In spite of this we have obtained a reasonable image (Figure 10) by brute force in the case at hand

8. Discussion and conclusion

The image shown in Figure 10 has many of the characteristics of a successful x-ray-microscope image and in particular is almost free of the oscillations due to the twin-image effect that are so evident in the image obtained from just a single backpropagation (Figure 6). Nonetheless we do not yet regard such images as ready for use in scientific applications of x-ray holography, although they certainly represent encouraging progress toward that. Our studies continue on how to improve the speed and accuracy of our reconstruction procedures.

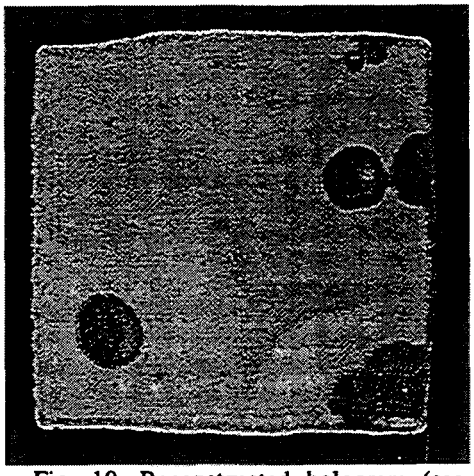

Fig. 10. Reconstructed hologram (see Fig. 5) with the twin-image suppression algorithm applied. The twin-image has been substantially reduced in the clear regions but the algorithm has not converged for regions inside the objects.

We believe that the use of cryo imaging essentially solves the radiation-damage problem and opens the way to multiview tomography. This raises the intriguing possibility that for a reasonably large number of views the twin-image signal may be *automatically* suppressed, as is found in certain types of electron holography.[16]

9. Acknowledgments

We thank J. Maser for working with us on parallel development of the cryo-sample holder and interface. We thank S. Wirick for providing technical assistance and A. Osanna for providing assistance with the cryo setup at beamline X1A at the NSLS. We acknowledge useful discussions with R. Glaeser and J. Kirz. This research was supported in part by the Alexander Hollaender Distinguished Postdoctoral Fellowship Program (SL) sponsored by The US Dept. of Energy (DOE), Office of Health and Environmental Research, and administered by the Oak Ridge Institute for Science and Education, by the DOE under

grant DE-FG02-89ER60858, Presidential Faculty Fellow award RCD 92-53618 (CJ), and Computational Science Graduate Fellowship Program (BC) sponsored by the DOE, and administered by Ames Laboratory. Holography exposures were carried out at the NSLS at Brookhaven National Laboratory, which is supported by the DOE.

10. References

1. Aikawa, M., "Variations in structure and function during the life cycle of malarial parasites", *Bull. WHO*, **55**, 139 (1977).
2. Baltes, H. P., ed., *Inverse Source problems*, Vol. 9, Springer Series in Topics in current physics, Berlin, 1978.
3. Dainty, J. C., J. R. Fienup, "Phase retrieval and image reconstruction for astronomy", in *Image Recovery: Theory and Application*, Stark, H., (Ed), Academic Press, Orlando, 1987.
4. Echlin, P., *Low-Temperature Microscopy and Analysis*, Plenum, New York, 1992.
5. Fienup, J. R., "Iterative Method Applied to Image Reconstruction and to Computer-generated Holograms", *Opt. Eng.*, **19**, 297-305 (1980).
6. Gerchberg, R. W., W. O. Saxton, "A practical algorithm for the determination of phases from image and diffraction plane pictures", *Optik*, **25**, 237-246 (1972).
7. Goodman, J. W., *Statistical Optics*, John Wiley, San Francisco, 1985.
8. Hadley, G., *Linear Algebra*, Addison-Wesley, Reading, USA, 1961.
9. Jacobsen, C., M. R. Howells, J. Kirz, K. McQuaid, S. Rothman, "X-ray Holographic Microscopy: Improved Image of Zymogen Granules", in *Short Wavelength Coherent Radiation: Generation and Applications*, Kirz, J., R. Falcone, (Ed), Vol. **2**, Optical Society of America Conference Proceddings, Washington, 1988.
10. Jacobsen, C., M. R. Howells, J. Kirz, S. Rothman, "X-ray Holographic Microscopy Using Photoresists", *J. Opt. Soc. Am.*, **A7**, 1847-1861 (1990).
11. Jacobsen, C. J., *X-ray Holography: a History*, Japan Scientific Societies Press, Springer Verlag, Tokyo, 1990.
12. Joyeux, D., S. Lowenthal, F. Polack, A. Bernstein, "X-ray Microscopy by Holography at LURE", in *X-ray Microscopy II*, Sayre, D., M. R. Howells, J. Kirz, H. Rarback, (Ed), Vol. **56**, Springer Series in Optical Sciences, Berlin, 1988.
13. Kilejian, A., A. Abati, W. Trager, "Plasmodium falciparum and Plasmodium coatneyi: immunogenicity of "knob-like protrusions" on infected erythrocyte membranes", *Exp. Parasitol.*, **42**, 157 (1977).
14. Koren, G., F. Polack, D. Joyeux, "Iterative Algorithms for Twin-Image elimination in in-line holography using finite support constraints", *J. Opt. Soc. Am*, **10**, 423-433 (1993).
15. Kurt Leskar, 1515, Worthington Ave, Clairton PA USA.
16. Len, P. M., S. Thevuthasan, C. S. Fadley, A. P. Kaduwela, M. A. V. Hove, "Atomic imaging by x-ray fluorescence holography and electron emission holography: a comparative theoretical study", *Phys. Rev. B*, **50**, 275-278 (1994).
17. Levi, A., H. Stark, "Restorations from phase and magnitude by generalized projections", in *Image Recovery: Theory and Application*, Stark, H., (Ed), Academic Press, Orlando, 1987.
18. Lindaas, S., M. Howells, C. Jacobsen, A. Kalinovsky, "X-ray holographic microscopy by means of photoresist recording and atomic-force microscope readout", *J. Opt. Soc. Am. A*, **13**, 1788-1800 (1996).
19. Lindaas, S., C. Jacobsen, M. R. Howells, "Development of a Linear Scanning Force Microscope for X-ray Gabor Hologram Readout", in *X-ray Microscopy*, Jacobsen, C., J. Trebes, (Ed), Proc SPIE, Vol. **1741**, Bellingham, 1992.
20. Lindaas, S. A., "X-ray Gabor Holography using a Scanning Force Microscope", Ph.D. Thesis, State University of New York at Stony Brook University, 1994.
21. Luse, S. A., L. H. Miller, "Plasmodium falciparum malaria. Ultrastructure of parasitized erythrocytes in cardiac vessels", *Am. J. Trop. Med. Hyg.*, **20**, 655 (1971).

22. Maleki, M. H., A. J. Devaney, "Noniterative reconstruction of complex-valued objects from two intensity measurements", *Opt. Eng.*, **33**, 3243-3253 (1994).
23. McNulty, I., J. Kirz, C. Jacobsen, E. Anderson, D. Kern, M. Howells, "High-resolution imaging by Fourier transform x-ray holography", *Science*, **256**, 1009-1012 (1992).
24. Meyer-Ilse, W., H. Medecki, J. T. Brown, J. Heck, E. Anderson, C. Magowan, A. Stead, T. Ford, R. Balhorn, C. Petersen, D. T. Attwood, "X-ray Microscopy at Berkeley", in *X-ray Microscopy and Spectromicroscopy*, Thieme, J., G. Schmahl, E. Umbach, D. Rudolph, (Ed), Springer Verlag, Heidelberg, 1996.
25. Pasvol, G., R. J. M. Wilson, M. E. Smalley, J. Brown, "Separation of viable schizont-infected red cells of Plasmodium falciparum from human blood", *Ann. Trop. Med. Parasitol.*, **72**, 87 (1978).
26. Saxton, W. O., *Computer Techniques for Image Processing in Electron Microscopy*, Academic Press, New York, 1978.
27. Schulz, M. S., H. Daido, K. Murai, Y. Kato, R. Kodama, G. Yuan, S. Nakai, K. Shinohara, I. Kodarma, T. Honda, H. Iwasaki, T. Yoshinobu, D. Neely, G. Slark, "Soft X-ray Holography using an X-ray Laser at 23.2/23.6nm and 19.6nm", in *Optical Society of America Topical Meeting; Shortwavelength V, San Diego*, Optical Society of America, Washington, 1993.
28. Snigirev, A., I. Snigireva, V. Kohn, S. Kuznetsov, I. Schelokov, "On the possibilities of x-ray phase contrast microimaging by coherent high-energy synchrotron radiation", *Rev. Sci. Instrum.*, **66**, 5486-5492 (1995).
29. Trager, W., J. Jensen, "Human maleria parasites in continuous culture", *Science*, **193**, 673 (1976).
30. Trager, W., M. A. Rudzinska, P. C. Bradbury, "The fine structure of Plasmodium falciparum and its host erythrocytes in natural malaria infections in man", *Bull. WHO*, **35**, 883 (1966).
31. Trebes, J. E., S. B. Brown, E. M. Campbell, D. C. Mathews, D. G. Nilson, G. F. Stone, D. A. Whelan, "Demonstration of X-ray Holography with an X-ray Laser", *Science*, **238**, 517-519 (1987).
32. Turcu, I. C. E., I. N. Ross, M. S. Schulz, H. Daido, G. J. Tallents, J. Krishnan, L. Dwivedi, A. Hening, "Spatial coherence measurements and x-ray holographic imaging using laser-generated plasma x-ray source in the water window spectral region", *J. Appl. Phys.*, (1993).
33. Wang, S., C. J. Jacobsen, "A numerical study of resolution and contrast in soft x-ray contact microscopy", in *X-ray Microscopy and Spectromicroscopy*, Thieme, J., G. Schmahl, E. Umbach, D. Rudolph, (Ed), Springer Verlag, Heidelberg, 1996.
34. Watanabe, N., K. Sakurai, A. Takeuchi, S. Aoki, "Soft x-ray Gabor in-line holography using CCD camera", in *X-ray Microscopy and Spectromicroscopy*, Thieme, J., G. Schmahl, E. Umbach, D. Rudolph, (Ed), Springer Verlag, Heidelberg, 1996.
35. Youla, D. C., "Mathematical theory of image restoration by the method of projections on to convex sets", in *Image Recovery: Theory and Application*, Stark, H., (Ed), Academic Press, Orlando, 1987.
36. Youla, D. C., H. Webb, "Image reconstruction by method of convex projections: Part 1-theory", *IEEE Trans. Medical Imaging*, **1**, 81-94 (1982).

Ernest Orlando Lawrence Berkeley National Laboratory
One Cyclotron Road | Berkeley, California 94720

Prepared for the U.S. Department of Energy under Contract No. DE-AC03-76SF00098